Journal of Civil Structural Health Monitoring (2021) 11:315–336
https://doi.org/10.1007/s13349-020-00454-9

ORIGINAL PAPER

A methodology to design measurement systems when multiple model classes are plausible

Numa J. Bertola[1,2] · **Sai G. S. Pai**[1] · **Ian F. C. Smith**[1,2]

Received: 15 June 2020 / Revised: 13 October 2020 / Accepted: 24 November 2020 / Published online: 7 January 2021

Abstract
The management of existing civil infrastructure is challenging due to evolving functional requirements, aging and climate change. Civil infrastructure often has hidden reserve capacity because of conservative approaches used in design and during construction. Information collected through sensor measurements has the potential to improve knowledge of structural behavior, leading to better decisions related to asset management. In this situation, the design of the monitoring system is an important task since it directly affects the quality of the information that is collected. Design of optimal measurement systems depends on the choice of behavior-model parameters to identify using monitoring data and non-parametric uncertainty sources. A model that contains a representation of these parameters as variables is called a model class. Selection of the most appropriate model class is often difficult prior to acquisition of information regarding the structural behavior, and this leads to suboptimal sensor placement. This study presents strategies to efficiently design measurement systems when multiple model classes are plausible. This methodology supports the selection of a sensor configuration that provides significant information gain for each model class using a minimum number of sensors. A full-scale bridge, The Powder Mill Bridge (USA), and an illustrative beam example are used to compare methodologies. A modification of the hierarchical algorithm for sensor placement has led to design of configurations that have fewer sensors than previously proposed strategies without compromising information gain.

Keywords Structural identification · Sensor placement · Model-class selection · Error domain model falsification · Joint entropy

1 Introduction

The global annual expenditure of the construction economy was recently evaluated at more than $10 trillion [1] and 30% of this is spent on civil infrastructure. As economic, environmental and material resources become increasingly scarce, more sustainable solutions for asset management are required. Fortunately, infrastructure often has reserve capacity due to safe construction and design practices. An accurate assessment of bridge reserve capacity requires predictions of structural behavior under actions. This behavior is influenced by several parameters, such as material properties and support conditions, that are difficult to estimate as characteristic values are not appropriate to assess existing structures [2].

The task of using field measurements to improve structural-model predictions is called structural identification [3]. Field measurements, collected through monitoring, help engineers improve reserve-capacity assessments of existing structures [4]. A model-based approach is usually necessary to compare aging-structure behavior with code-based load-carrying requirements [5]. Model-free approaches are only suitable to perform behavior interpolation and the emergence of anomalies such as structural damage [6].

The task of building behavior models, such as finite-element (FE) models, requires numerous assumptions, leading to several sources of uncertainties. Prior to measurements, engineers must select an appropriate model class that requires the selection of primary model parameters and the quantification of non-parametric uncertainties.

✉ Numa J. Bertola
numa.bertola@epfl.ch

[1] Future Cities Laboratory, Singapore-ETH Centre, ETH Zurich, 1 CREATE Way, CREATE Tower, Singapore 138602, Singapore

[2] Applied Computing and Mechanics Laboratory, EPFL, 1015 Lausanne, Switzerland

Due to the computational time to generate model predictions with a unique set of parameter values, the number of primary parameters used in the model class is limited [7]. Simple model classes, defined by few model parameters, often provide acceptable data interpretation [8]. Traditionally, primary-parameter selection has been carried out using sensitivity analysis based on linear-regression models [9, 10]. However, civil-infrastructure responses may not have a linear relationship with model parameters such as boundary conditions [11]. Recently, methods based on shrinkage [12] and clustering [13] have been introduced. A comprehensive review of feature-selection methods used in structural identification has been presented in [14].

Once the numerical model is built and the model class is selected, a data-interpretation methodology is needed to compare model predictions with field measurements. Most studies in the literature have chosen either a residual-minimization strategy or a Bayesian model updating (BMU) approach, see [15, 16] amongst others. Use of these methods usually requires the assumption that uncertainties have zero-mean independent Gaussian forms [17–19]. However, this hypothesis is usually not valid for civil infrastructure since several modelling assumptions, such as idealized boundary conditions and model fidelity, imply systematic uncertainties [20]. Although modifications to traditional implementations of BMU have been proposed to meet this challenge, they lead to complex formulations that are difficult to validate [21, 22]. A new structural-identification methodology called error-domain model falsification (EDMF) has been proposed that is easy to use for engineers [23]. This methodology is based on the concept of falsification by Popper [24], where scientific hypotheses cannot be verified with data; they can only be refuted. EDMF has been shown empirically and theoretically to be equivalent to a modified Bayesian model updating methodology where the likelihood function is defined by a L∞-norm-based Gaussian function [22].

In EDMF, a set of model instances with unique parameter values are first generated using a finite-element model. Then model-instance predictions are compared with field measurements (sensor data). Model instances are falsified if discrepancies between predictions and sensor data cannot be explained by uncertainties given a level of confidence. Deciding upon levels of confidence at the beginning is standard engineering practice for evaluation of critical limit states. For example, this is how safety factors are fixed.

When a model instance is falsified, this means that its combination of parameter values is not possible, while all accepted model instances are assigned an equivalent probability of having the true parameter values. By falsifying model instances, information is thus gained, and ranges of plausible parameter values are reduced.

Systematic uncertainties are explicitly represented in a way that is compatible with practical engineering knowledge [25], as no blackbox tools and complex statistical knowledge are required. While practicing engineers do typically have an idea of bounds on variable values, they usually do not know what the values are for mean and standard deviation. Furthermore, for some important sources of uncertainty, such as model fidelity and boundary conditions, a normal distribution cannot be justified [5]. EDMF has been shown to provide accurate (avoiding wrong identification) model-parameter identification when compared with traditional BMU [25] in the presence of systematic bias. Identification with EDMF is often less precise as parameter values are identified through bounds of model-parameter values. A uniform distribution is typically assumed between these bounds [23].

The performance of structural identification depends on the choice of the measurement system, which is composed of a sensor configuration and excitations [26]. The measurement system is usually designed using only engineering judgement along with basic metrics such as signal-to-noise ratio [27]. The quantitative design of measurement systems has recently attracted much research interest. Optimization strategies used for measurement-system design require the selection of an objective function to assess sensor locations and an optimization strategy to ensure reasonable computational times [28]. Since the computational complexity of the general sensor-placement algorithm is exponential with respect to the number of sensors [29], researchers have used greedy algorithms (sequential search) to reduce the computational effort of sensor placement [30].

Most recent studies have focused on the best objective function for measurement-system design. Several approaches that involve either minimizing the information entropy in posterior model-parameter distributions [26, 31] or maximizing information entropy in multiple-model predictions have been proposed [32, 33]. In these approaches, sensor locations have been ranked based on their ability to assess model-parameter values. Other researchers have used modal properties to estimate sensor utility for structural identification based on Fisher Information Matrix [34], modal assurance criterion [35], frequency–response functions [36] and a combination of above-mentioned criteria [37]. Nevertheless, these metrics can only be used for dynamic load testing, while entropy-based metrics, such as the approach used in this paper, are also applicable to static load tests.

Once the first sensor location has been selected, the redundancy of information gain between sensors during optimization has often been neglected in studies involving entropy-based metrics for measurement-system design, leading to sensor clustering issues [38]. To meet this challenge, information-entropy values of neighboring sensors have been arbitrarily reduced [39]. Another strategy has been to use global-search algorithms, such as Genetic algorithms [40–42] and Particle Swarm Optimization [43, 44]. However,

these strategies have required large amounts of computational time to determine optimal sensor configurations.

Joint entropy has been introduced as an objective function for measurement-system design to explicitly account for mutual information between sensors [45]. The hierarchical algorithm, that combines a greedy search with the joint-entropy objective function, has successfully been applied to studies of wind around buildings [46]. This algorithm has also been adapted for structural identification to include mutual information among static load tests [47] and dynamic load tests [48]. For structural identification, the hierarchical algorithm has shown to find near-optimal solutions while reducing significantly the computational time compared with global-search approaches [49].

Several researchers (for example, [32, 38, 50]) have observed that the optimal measurement system depends on the choice of model parameters for identification and non-parametric uncertainty sources. A model that contains a representation of these parameters as variables is called a model class. A model class must thus be selected prior to monitoring to design effectively the measurement system [51]. However, structural identification has been shown to be an iterative rather than linear process [52]. This means that often, the appropriate model class is known only after sensor data have been collected. In such situations, the initial design of measurement systems is often suboptimal, limiting the potential for information gain. When engineers consider several plausible model classes prior to monitoring, this information should be included in the measurement-system design.

Papadimitriou [53] proposed a methodology that selects sensor locations based on a Pareto optimization between model classes. As this methodology uses information entropy (not joint entropy) as a sensor-placement objective function, a lack of shared-information analyses may lead to sensor clustering. No methodology is available to design measurement systems when multiple model classes are plausible that explicitly accounts for the mutual information between sensors.

This paper proposes and compares two methodologies to design measurement systems for multiple model classes. In the first method, referred to as the traditional approach, the measurement system is designed for each model class independently. Then the final configuration includes sensors that are useful for at least one model class. The second methodology introduces a modification of the hierarchical algorithm to find the optimal sensor configuration based on the information from all model classes. Using the second methodology, configurations with fewer sensors are obtained without compromising the potential for information gain.

The paper is organized as follows. First, background methodologies are presented in Sect. 2. Then two methodologies are introduced in Sect. 3 to design measurement systems when multiple model classes are plausible. Two case studies, a theoretical beam example and the Powder Mill Bridge are used to compare these methodologies (Sect. 4).

2 Background

In this section, background methodologies, that are necessary for understanding this study, are presented. First, the structural-identification methodology, called error-domain model falsification, is introduced. Then the hierarchical algorithm is described for a given model class.

2.1 Structural identification: error-domain model falsification

2.1.1 Presentation

Error-domain model falsification (EDMF) is a methodology for structural identification [23]. EDMF utilises a model class that includes parameters having the most important sources of uncertainties. They are quantified as random variables with a uniform prior probability density function (PDF). The posterior PDFs of these model parameters are found by comparing sensor measurement data with model predictions. Due to inherent lack of complete knowledge of uncertainties all solutions obtained with EDMF are assumed to be equally likely. These approximations are compatible with the quality of information that is typically available in real situations.

First, the model class is chosen. The model class usually involves a finite-element parametric model that includes characteristics such as material properties, geometry, boundary conditions and excitations as well as the quantification of non-parametric-model (U_{i,g_k}) and measurement ($U_{i,y}$) uncertainties. Additionally, a set of critical model-parameter values that can be identified are selected and possible ranges (uniform prior distributions) of parameter values are estimated. Then, a population of model instances is generated, where each instance has a unique combination of model-parameter values. By comparing model-instance predictions with each field measurement independently (without correlation assumptions), EDMF helps identify plausible model instances among the initial population.

In EDMF, a model instance is falsified if its prediction lies outside threshold bounds for at least a sensor location. This methodology is robust to wrong estimations of correlation between sensor data as EDMF uses hyper-rectangular projections for threshold values [23]. The solutions (candidates) of EDMF define the posterior PDF of these model parameters. Due to inherent lack of complete knowledge of uncertainties affecting the inverse task, all solutions obtained with EDMF are assumed to be equally likely. Therefore,

uniform distributions between model-parameter bounds are typically assumed.

2.1.2 Mathematical framework

Model-instance predictions $g_i(\Theta_k)$ at sensor location i are generated by assigning a unique set of parameter values Θ_k for the model class k. The true structural response R_i, that is unknown in practice, is linked to the field measurements y_i and model prediction $g_i(\Theta_k)$ using Eq. (1), where n_y is the number of monitored sensor locations.

$$g_i(\Theta_k) + U_{i,g_k} = R_i = y_i + U_{i,y} \forall i \in \{1, \ldots, n_y\}. \quad (1)$$

Using Monte Carlo sampling, model U_{i,g_k} and measurement $U_{i,y}$ uncertainties are combined in a unique source of combined uncertainty $U_{i,c}$. Following [54], Eq. (1) is then transformed to Eq. (2). The residual r_i quantifies the discrepancy between the model prediction and the field measurement at sensor location i.

$$g_k(i, \Theta_k) - y_i = U_{i,c} = r_i. \quad (2)$$

In EDMF, plausible instances are selected by falsifying models that have residuals larger than defined threshold bounds. These thresholds are calculated using combined-uncertainty distributions and a target reliability of identification ϕ. Traditionally, this target ϕ equals to 95% [23] and the Šidák correction [55] is used to maintain a constant level of confidence when multiple comparisons are performed between field measurements and model-instance predictions (several sensor locations). Then threshold bounds, $t_{i,low}$ and $t_{i,high}$, are evaluated (Eq. 3). These bounds are calculated as the shortest intervals through the PDF of combined uncertainties $f_{U_i}(u_i)$ at sensor location i.

$$\forall i = 1, \ldots, n_y : ^{1/n_y} = \int_{u_{i,low}}^{u_{i,high}} f_{U_i}(u_i) du_i. \quad (3)$$

The candidate model set (CMS)Ω_k'', defined using Eq. (4), is built of non-falsified model instances.

$$\Omega_k'' = \{\theta_k \in \Omega_k | \forall i \in \{1, \ldots, n_y\} t_{i,low} \leq g_k(i, \Theta_k) - \hat{y}_i \leq t_{i,high}\}. \quad (4)$$

These instances are assumed to be equivalent since little information is usually available to describe the combined-uncertainty distribution [54]. They are thus assigned an equal probability, while falsified model instances are assigned a null probability.

In the case that all model instances are falsified, model predictions are incompatible with measurements given the estimations of non-parametric uncertainty sources. Therefore, the current model class is not compatible with the true structural behavior. In such cases, data interpretation using EDMF leads to re-evaluation of assumptions related to the choice of model class and uncertainty quantification. This situation highlights an important advantage of EDMF compared with other structural-identification approaches [52]. These approaches, such as BMU or residual minimization, may yield updated parameter values even when incorrect assumptions are made prior to the structural identification, leading to wrong identification [25].

2.2 Hierarchical algorithm

A measurement-system-design framework is used to rationally select the appropriate measurement system to maximize information gain. This information gain is evaluated by the ability of a measurement system to discriminate model instances based on their predictions at sensor locations. The aim is to find the measurement that will maximize the number of falsified model instances to reduce parameter-value ranges after monitoring.

Due to the large number of possible combinations of sensor configurations, sensor placement is an optimization task, where a greedy-search algorithm is typically used [26]. Information entropy has been introduced as the variable in a sensor-placement objective function for system identification in posterior parameter distributions [31] and model-instance prediction distributions [32]. In EDMF context, this objective function measures the variability of model-instance predictions at sensor locations and aims to find the location that maximizes the discrimination of model instances.

To evaluate this variability, a prediction histogram is generated at each sensor location i. The range of model-instance predictions are subdivided into $N_{I,i}$ intervals where the interval width is given by combined uncertainty $U_{i,c}$ (Eq. 2). The probability that the model-instance prediction $g_{i,j}$ falls inside the jth interval is equal to $P(g_{i,j}) = m_{i,j} / \sum m_{i,j}$ with $m_{i,j}$ the number of model instances falling inside this specific interval. The information entropy $H(g_i)$ of sensor location i is then evaluated using the following equation:

$$H(g_i) = -\sum_{j=1}^{N_{I,i}} P(g_{i,j}) \log_2 P(g_{i,j}). \quad (5)$$

As information entropy measures the disorder in predictions, sensor locations associated with large information-entropy values represent a high potential for model-instance discrimination. Therefore, they are attractive sensor locations.

When systems of elements, such as bridges, are monitored, measurements between sensor locations are typically correlated. Therefore, selecting locations only based on their information-entropy values leads to redundant measurement systems [47]. To account for the mutual information between locations, joint entropy has been introduced as a new variable in the objective function for sensor placement [45].

Joint entropy $H(g_{i,i+1})$ evaluates the information entropy amongst sets of predictions at sensor locations. For a set of two sensors, joint entropy is calculated using Eq. (6), where $P(g_{i,j}, g_{i+1,k})$ is the joint probability that model-instance predictions fall inside the jth interval at sensor i and the kth interval at sensor $i+1$. In this equation,$k \in \{1, \ldots, N_{I,i+1}\}$ and $N_{I,i+1}$ is the maximum number of prediction intervals at the i + 1 location and $i+1 \in \{1, \ldots, n_s\}$ with the number of potential sensor locations n_s.

$$H(g_{i,i+1}) = -\sum_{k=1}^{N_{I,i+1}} \sum_{j=1}^{N_{I,i}} P(g_{i,j}, g_{i+1,k}) \log_2 P(g_{i,j}, g_{i+1,k}). \tag{6}$$

Due to the redundancy in information gain between sensors, the joint entropy is less than or equal to the sum of the individual information entropies at sensors i and $i+1$. Equation (6) can be changed to Eq. (7), where $I(g_{i,i+1})$ is the shared information between sensor locations i and $i+1$.

$$H(g_{i,i+1}) = H(g_i) + H(g_{i+1}) - I(g_{i,i+1}). \tag{7}$$

The sensor-placement algorithm that uses this variable has been adapted to structural identification to take into account mutual information between static load tests [47] as well as dynamic data [48]. Additionally, a measurement-system-design strategy has been proposed following a multi-criteria decision analysis where the information-gain is evaluated using joint entropy [51].

3 Measurement-system design when multiple model classes are plausible

In this section, two methodologies are introduced to design measurement systems when multiple model classes are plausible. The first approach involves an independent measurement-system design for each model class and then a combination of these independent sensor configurations. Although this approach has not been yet formalized, it is referred to in this paper as the traditional approach to design measurement systems for multiple model classes. The second methodology involves a modification of the hierarchical algorithm (Sect. 2.2) to account for the information gain for all model classes.

3.1 Traditional approach

3.1.1 Methodology

In this section, the traditional methodology to design measurement systems for multiple model classes is developed. This methodology involves a combination of the optimal measurement system for each model class.

Figure 1 presents the flowchart of the traditional approach for measurement-system design when multiple model classes are plausible. First, the numerical model of the structure is built based on available information and site investigation. Possible monitoring systems, such as possible sensor types and locations and possible load tests, are defined. Then, the model class must be selected, including a small set of model parameters than can be identified using sensor data during load testing and the non-parametric uncertainties associated with this choice. This choice is usually not trivial and often it appears that the initial model class is incorrect, leading to an iterative process of structural identification [52]. In this study, it is assumed that engineers are unable to select one model class; several model classes (MCi) are possible.

In Fig. 1, although three classes are included in the flowchart as an example, the methodology can be used with any number of model classes. The optimal measurement system for each model class is then defined. For each model class, the hierarchical algorithm (Sect. 2.2) is run to obtain an optimal sensor configuration. This task is described in detail below. Finally, the optimal sensor configuration for multiple model classes is taken as the union of all sensor configurations. Thus, sensor locations that are at least useful for one model class are included in the final sensor configuration.

3.1.2 Optimal sensor configuration for a given model class

For a given model class, the optimal sensor configuration is obtained using the hierarchical algorithm. The model-instance predictions at possible sensor locations are used to find locations that maximize the joint entropy (Eq. 6). A ranking of sensor locations is thus obtained and an evaluation of the information gain (joint entropy) is provided with respect to the number of sensors, as shown in Fig. 2 for two model classes. According to user preferences, a target of information gain is set for each model class, for example 80% or 100%. The optimal number of sensors is then found for each model class. The selected configuration is defined according to the sensor-location ranking of the hierarchical algorithm. A higher target leads to a larger number of sensors in configurations and thus more expensive monitoring systems. As the cost of monitoring and information gain metrics are typically conflicting, the ultimate choice is based on preferences as well as characteristics of the optimal solutions [51].

Joint-entropy curves for various model classes may be significantly different and thus, the optimal number of sensors as well as their locations may vary (Fig. 2a, b). If these sensor configurations are simply combined through taking the union of the two sensor sets, a large number of sensors are included in the configuration. Since many sensors may provide similar information, the risk of information redundancy is high due to mutual information gain.

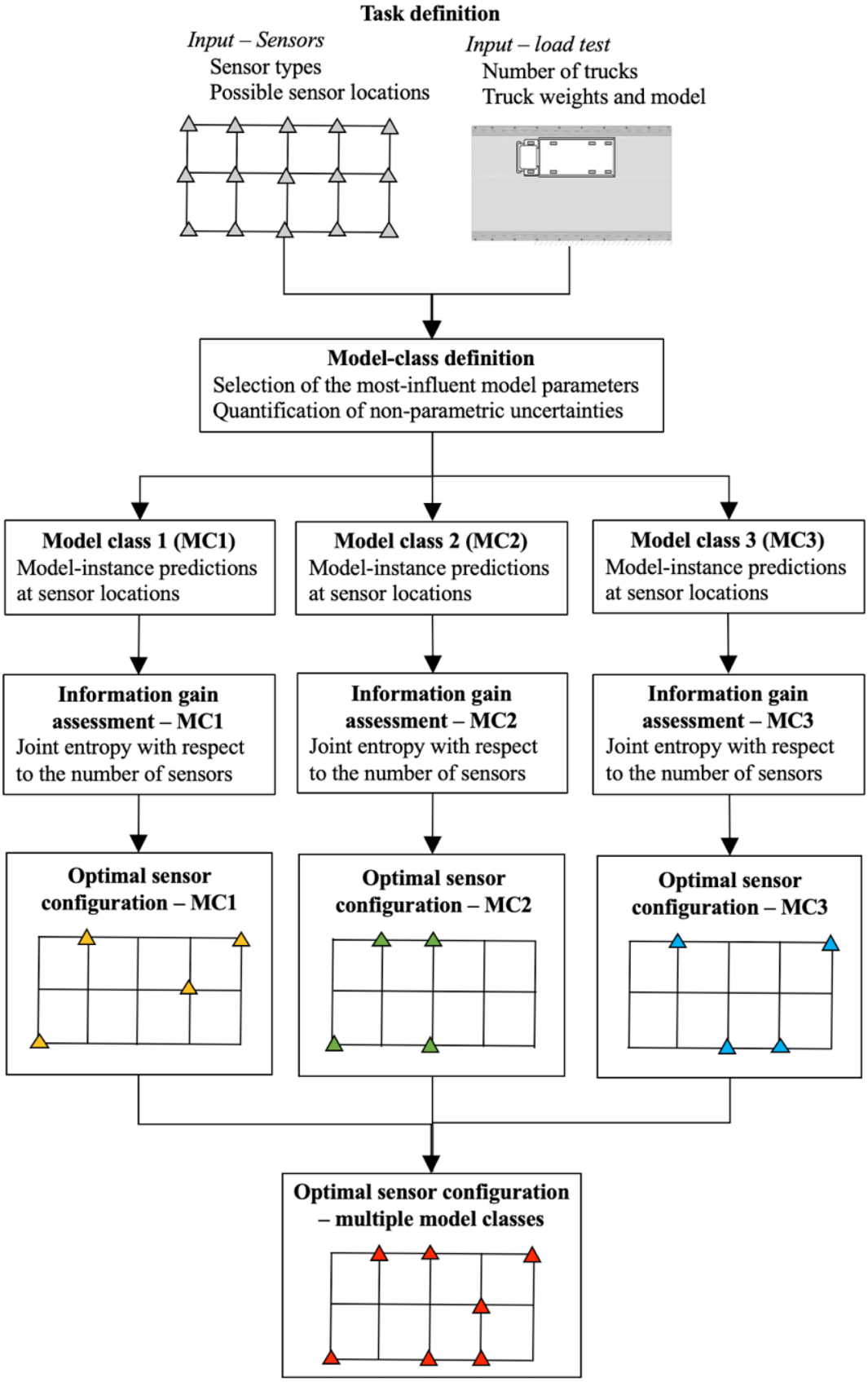

Fig. 1 Flowchart of the traditional approach for measurement-system design when multiple model classes are plausible

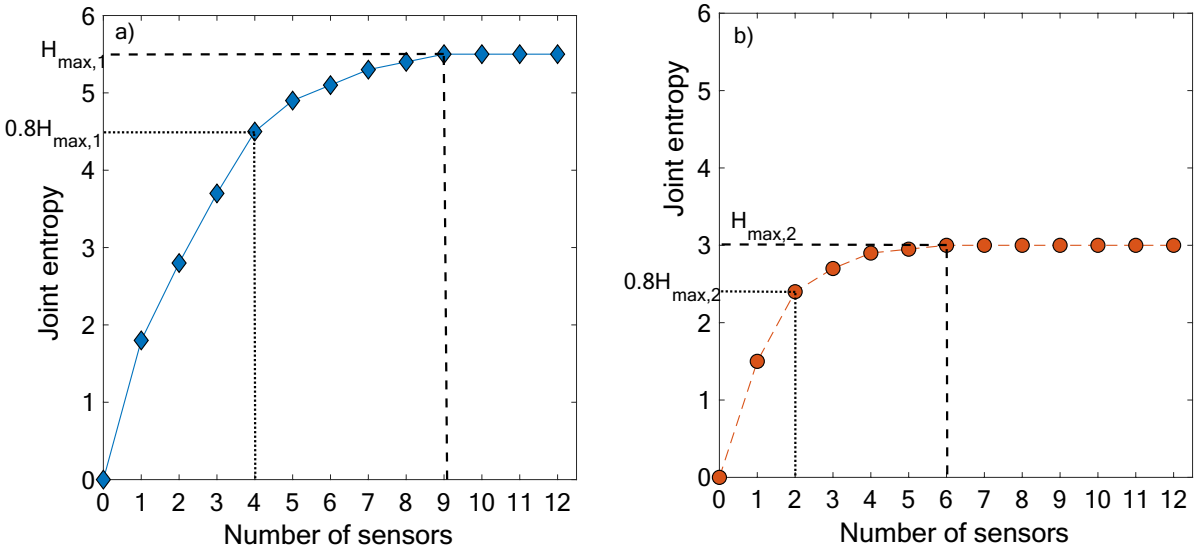

Fig. 2 Example of joint-entropy evaluation as a function of the number of sensors for two model classes. **a** Model class 1; **b** model class 2

3.2 Modified hierarchical algorithm for multiple model classes

The second methodology involves a modification of the hierarchical algorithm (Sect. 2.2) to account for information related to use of multiple model classes for sensor placement. First, the flowchart of the methodology is presented. Then, the modification of the joint-entropy objective function (Eq. 7) is introduced and the definition of the optimal sensor configuration is described.

3.2.1 Flowchart

Figure 3 is a flowchart of the modified hierarchical algorithm for multiple model classes. First, the numerical model of the structure is built and possible monitoring systems are defined. In a similarly way to the traditional approach (Fig. 1), possible model classes are selected. The main difference from the previous method is that the measurement system is designed based on information from all model classes to find sensor locations that maximize the mean information gain in each model class. This part of the flowchart is discussed in Sect. 3.2.2. Using a target for the total information gain chosen by asset managers, the optimal sensor configuration is defined. Then, a verification is made to guarantee that the selected sensor configuration provides the required information gain for each model class independently. When this verification is not satisfied, an additional sensor is added to the sensor configuration following the hierarchical algorithm (Sect. 2.2). When the target of information gain is reached for each model class, the optimal sensor configuration for multiple model classes is obtained.

3.2.2 Modification of the hierarchical algorithm

In this section, the modification of the hierarchical algorithm is introduced. The improvement with respect to the original hierarchical algorithm (Sect. 2.2) and this algorithm is the objective function. The aim of this modification is to account for the information gain of sensor locations in all model classes for sensor placement. Joint entropy is simultaneously evaluated in both model classes and the location that has the largest mean value is selected. This sensor location thus provides the largest additional information gain in both model classes.

The joint-entropy function of the hierarchical algorithm (Eq. 6) is modified to account for the mean information gain of a sensor location in both model classes. Equation (8) presents the new joint-entropy objective function, where $\widehat{H}_j(g_i)$ is the normalized joint entropy of location i for the model class j and $j \in \{1, \ldots, N_{\mathrm{MC}}\}$ with $\mathrm{N_{MC}}$ is the number of model classes under consideration.

$$\bar{H}_i = \sum_{1}^{N_{MC}} \widehat{H}_j(g_i). \tag{8}$$

Figure 4 presents an illustrative example of sensor placement using the modified hierarchical algorithm. This example involves three possible locations and two plausible model classes, called MC1 and MC2. In the first iteration, all locations are evaluated for both model classes independently and mean values are computed. In this example, sensor location 2 has the largest mean entropy value ($\bar{H}_2 = 0.8$). Due to the greedy search strategy used by the hierarchical algorithm, only sensor configurations that include sensor location 2

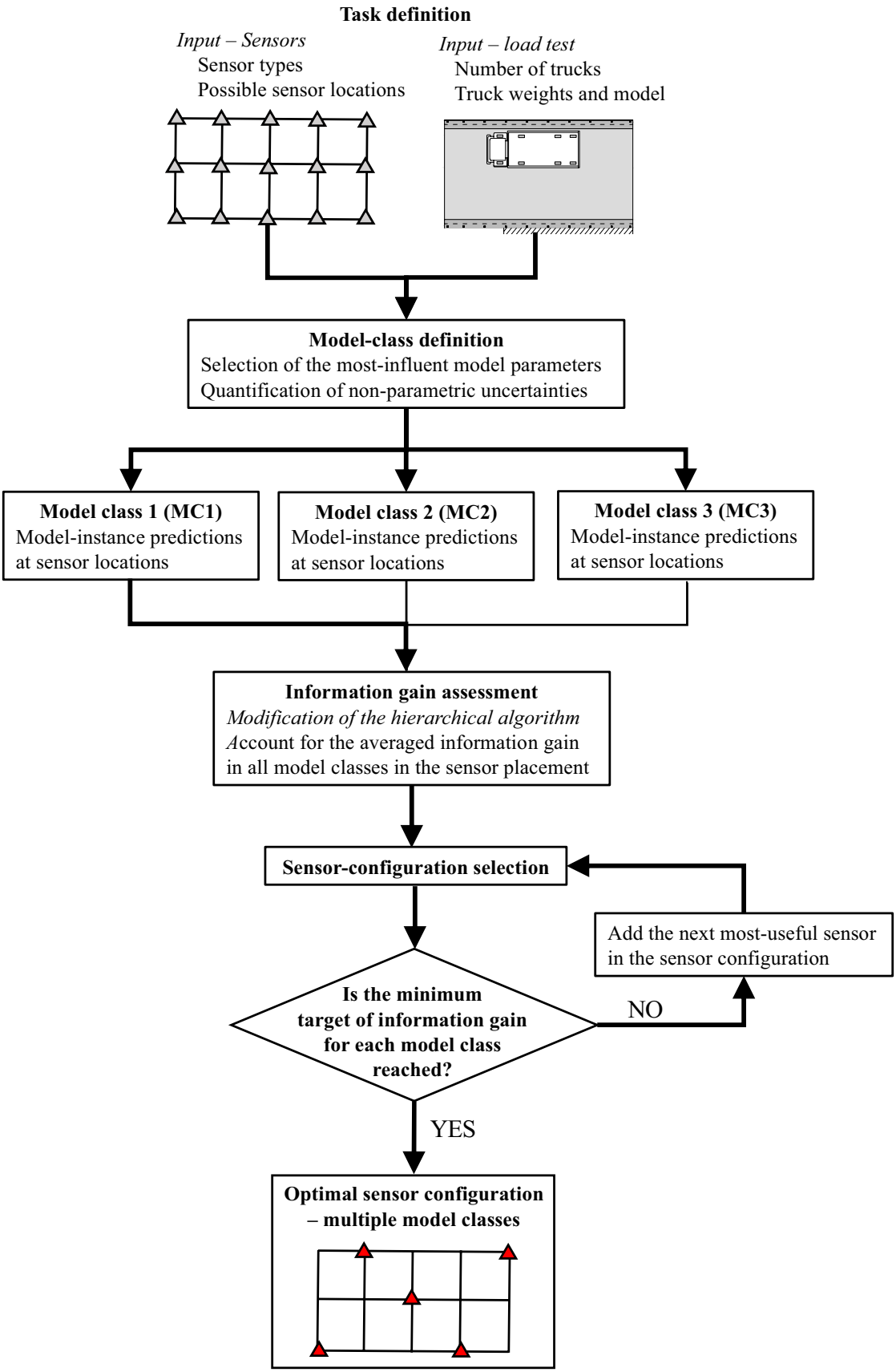

Fig. 3 Flowchart of the modified hierarchical algorithm for multiple model classes

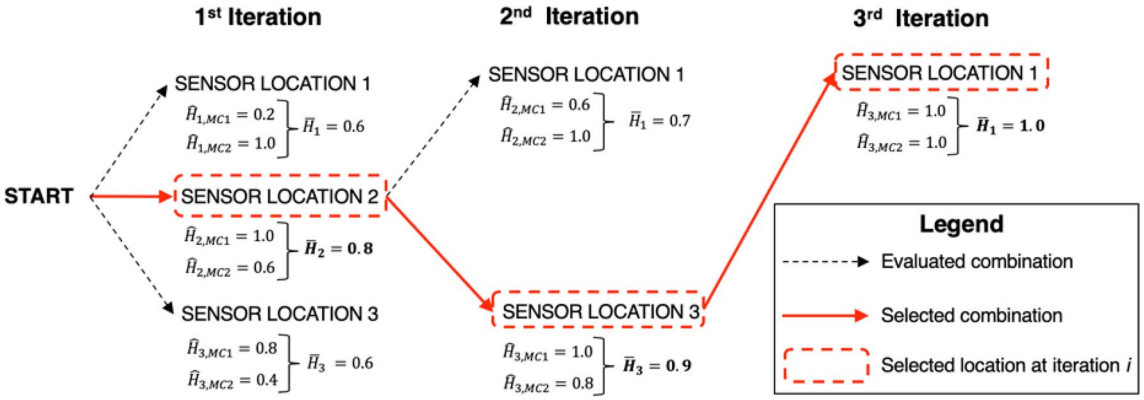

Fig. 4 Example of the sensor-location selection using the modified hierarchical algorithm

are re-evaluated in the second iteration. This means that the global optimum may not be found as the combination of sensor locations 1 and 3 is not assessed. Nevertheless, this sequential search significantly reduces computational time. The results approach the global optimum as the number of sensors increases. Finally, a good solution is ensured since the best individual sensor location is always included [56].

3.2.3 Optimal sensor configuration

Once the sensor ranking is obtained using the modified hierarchical algorithm, the optimal sensor configuration is defined to reach a target such as a minimum information gain (joint entropy). As the sensor-location ranking is known, the mean information gain with respect to the number of sensors can be easily obtained using Eq. (8) without normalizing joint-entropy values. The sensor configuration with the minimal number of sensors that satisfies the information-gain target is selected. Then a verification is made to ensure that this minimal information gain is obtained for each model class. If this verification is satisfied, the optimal sensor configuration is obtained. If the verification fails, additional sensors are added to the configuration following the ranking provided by the modified hierarchical algorithm (Fig. 4), until the target of information gain is reached for each model class independently.

4 Case study

Two case studies are introduced to illustrate scenarios when multiple model classes are plausible. In the simple-beam example (Sect. 4.1), the influence of the uncertainty quantification is presented, while in the Powder Mill Bridge, (Sect. 4.2) several model-parameter sets are introduced.

4.1 Theoretical example: simple beam

A theoretical example of a simple beam, similar to [25], is used to illustrate the influence of the non-parametric uncertainty quantification on the expected information gain of sensor configurations. Several model classes are proposed that differ in uncertainty magnitudes. Results are presented in terms of individual sensor performance, joint-entropy values of sensor configurations and sensor-location rankings. Expected performance scores of individual sensor locations and sensor configurations are compared with the information gain after simulated field measurements using EDMF (Sect. 2.1).

This example involves a simply supported prestressed concrete beam that is partially fixed on the left side by a rotational spring under a distributed load ($s = 5$kN/m) as presented in Fig. 5. This beam has a squared cross section of height $h = 500$ mm with a moment of inertia I and length $L = 10{,}000$ mm. Two characteristics are unknown prior to monitoring: the Young's modulus E and the spring rotational stiffness K. The monitoring goal is thus to identify as precisely as possible both parameter values.

Potential strain-gauge locations are uniformly distributed on the beam, starting at 1000 mm from the left side. The change in tensile strain at the bottom of the beam due to loading at the coordinate x is calculated using the following equation:

$$\varepsilon(x) = -\frac{s(L-x)[KL(L-4x) - 12EIx]}{8EI(3EI + KL)}h/2. \tag{9}$$

In this example, the aim of measurement-system design is to select sensor locations that maximize the information

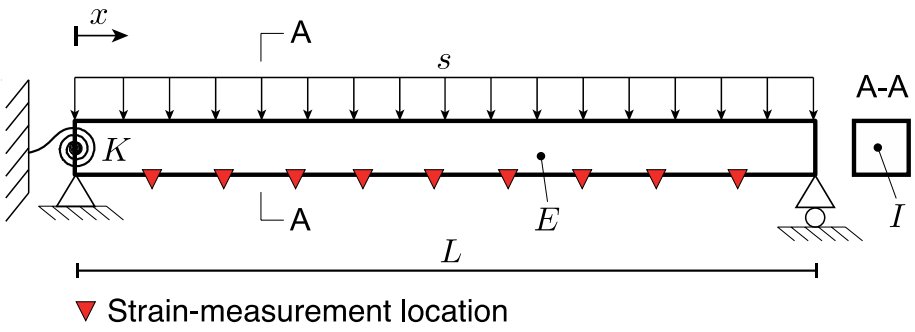

Fig. 5 Beam configuration with nine potential measurement locations ($n_S = 9$)

Table 1 Initial parameter ranges and ground-truth values

	Young's modulus E [GPa]	Rotational stiffness K [log(Nmm/rad)]
Initial parameter range	25–40	8–12
Ground truth	29	11.2

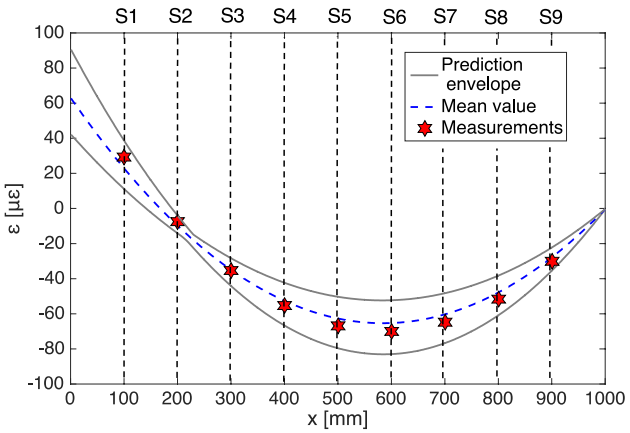

Fig. 6 Model-instance predictions at sensor locations with simulated measurements according to the beam parameter values

gain evaluated through the reduction of initial parameter ranges.

4.1.1 Model parameters

Table 1 presents the initial parameter ranges of both parameters as well as their true values (unknown in practice). True parameter values are assumed to simulate measurements at possible sensor locations. In this 2-parameter space, 961 model instances are generated using grid-based sampling. This initial population constitutes the input required for the sensor-placement algorithms as well as the initial model-instance set for falsification.

Table 2 Load-magnitude uncertainty scenario

Scenario	Distribution
No-uncertainty [%]	U[0; 0.1]
Normal uncertainty [%]	U[− 2; 5]
Large uncertainty [%]	U[− 5; 15]
Very large uncertainty [%]	U[− 25; 50]

Figure 6 presents model-instance predictions with respect to the distance from the left-side support of the beam. Extreme and mean values are shown as well as the simulated measurements at possible sensor locations due to the assumed parameter values where no uncertainties in the measurements have been included. Results show that parameter values significantly influence model-instance predictions. The aim of sensor placement is to optimize the sensor configuration to maximize the discrimination of model instances.

4.1.2 Model classes

In this section, several possible model classes are introduced. These model classes differ in the magnitude level of the distributed load applied on the beam. Table 2 contains four scenarios of uncertainty levels. The first scenario, called "no-uncertainty", involves a perfectly known loading level, while the high-uncertainty scenario includes loading uncertainties up to 50%. These scenarios are used to evaluate the influence of the uncertainty level on the optimal measurement system. Non-parametric model uncertainties are typically not centred on zero due to the nature of the model bias. For example, model simplifications such as boundary conditions and connections between structural elements are intended to be conservative rather than accurate [5]. In this beam example, uncertainty scenarios are thus chosen to be not centred on zero in a similar way to the full-scale case study, the Powder Mill Bridge (Sect. 4.2). These uncertainties are assumed to have uniform distributions between upper and lower bounds (U[lower, upper]).

Table 3 Non-parametric uncertainty sources—simple-beam example

Source	Distribution
Beam inertia I [%]	U[− 1;1]
Beam length L [%]	U[− 1;1]
Sensor accuracy [με]	U[− 2;2]

Table 3 presents additional modelling and measurement uncertainty sources involved in this example. These sources also have uniform distributions between the two bounds. Uncertainty sources on geometric properties are assumed to affect model-instance predictions by ± 1%. Additionally, strain gauges have sensor accuracies of ± 2 με. These uncertainties are applied to all model-class scenarios.

4.1.3 Expected information gain and identification for each model class

The expected information gain of individual sensors and sensor configurations is compared with the falsification performance using the ground-truth parameter values (Table 1) using the EDMF framework (Sect. 2.1) for data interpretation. The falsification performance is calculated as the ratio of falsified model instances over the total number of instances.

Figure 7 presents the sensor performance for each model-class scenario. The sensor performance is significantly influenced by its location. S1 presents the highest expected information gain for all model classes for the no-uncertainty scenario (Fig. 7a). This result shows that the variability of model predictions is more important than the signal-to-noise ratio (obtainable from Fig. 6). Higher uncertainty magnitudes significantly reduce individual sensor performance and this trend is observed for all sensor locations. These results are corroborated by the individual falsification performance of sensor location (Fig. 7b) using ground-truth parameter values.

Figure 8 presents the information gain with respect of the number of sensors in the sensor configuration for each model-class scenario based on the sensor-location rankings obtained with the hierarchical algorithm (Sect. 2.2). The expected information gain is significantly influenced by the model-class scenario (Fig. 8a) as higher uncertainty-level magnitudes drastically reduce the model-instance discrimination (Fig. 8b). Additionally, the number of sensors to reach the maximum joint-entropy values varies from 1 sensor for the very high uncertainty scenario to 9 sensors to the no-uncertainty scenario. This result shows that the choice of the model class may lead to a various optimal measurement systems. However, the number of useful sensors in terms of falsification performance is bounded between 1 and 5 depending on the model class (Fig. 8b).

Figure 9 presents the sensor-location ranking for each model class independently. Results are presented as a histogram with polar coordinates from the first sensor location selected to the last one. Sensor rankings significantly differ with the model class selected. For example, S7 is ranked as the third-best location for the no-uncertainty and very large uncertainty scenarios and as the worst location for the normal and large uncertainty scenarios. This result shows once more that the optimal sensor configuration is influenced by the model class.

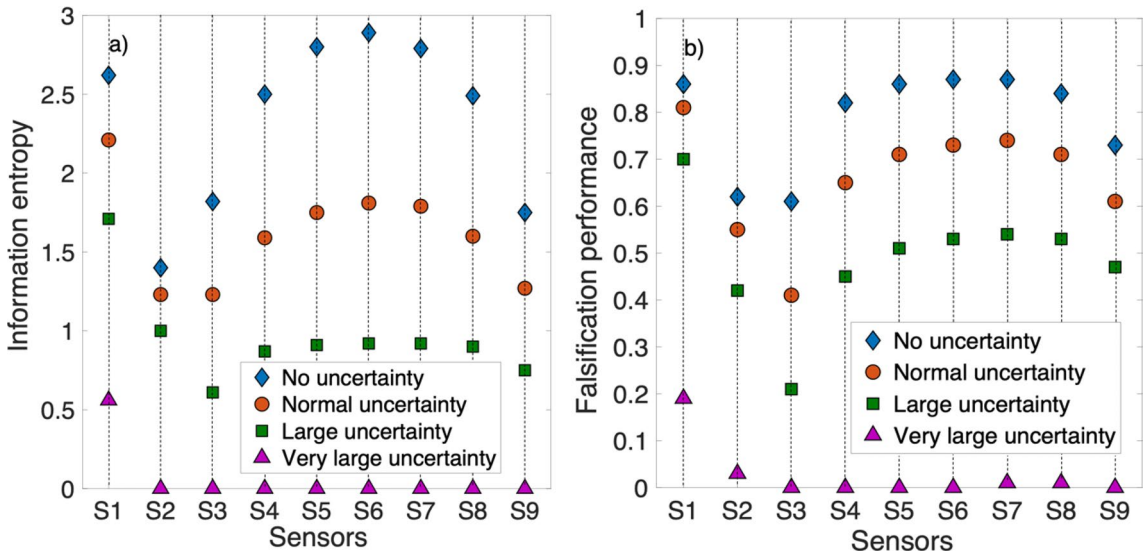

Fig. 7 Comparison of information gain and identification performance of individual sensors for the four model classes. **a** Information entropy; **b** falsification performance

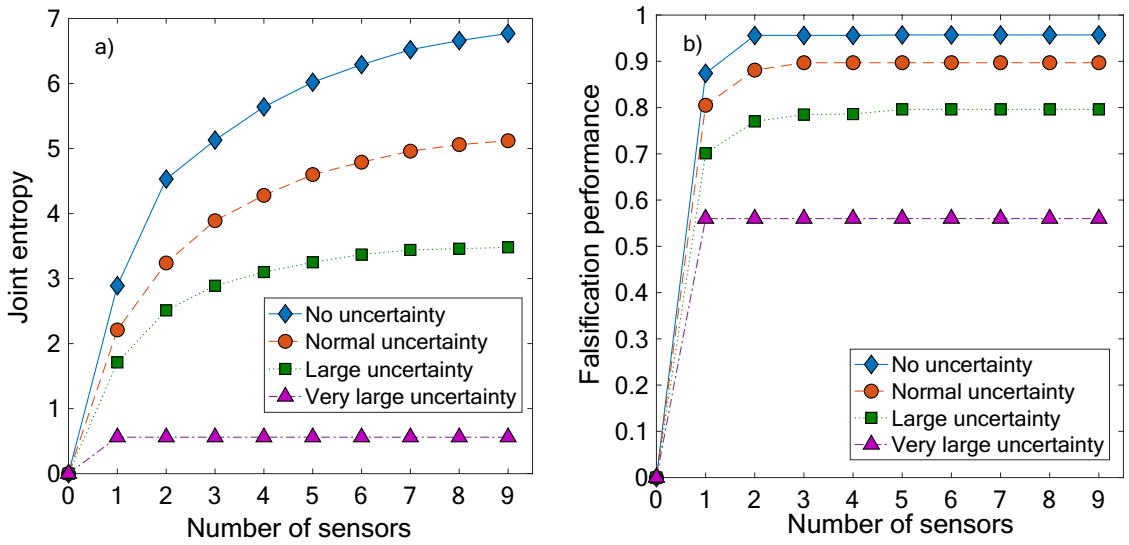

Fig. 8 Comparison of information gain and identification performance with respect to the number of sensors for the four model classes for the simple-beam example. **a** Joint entropy; **b** falsification performance

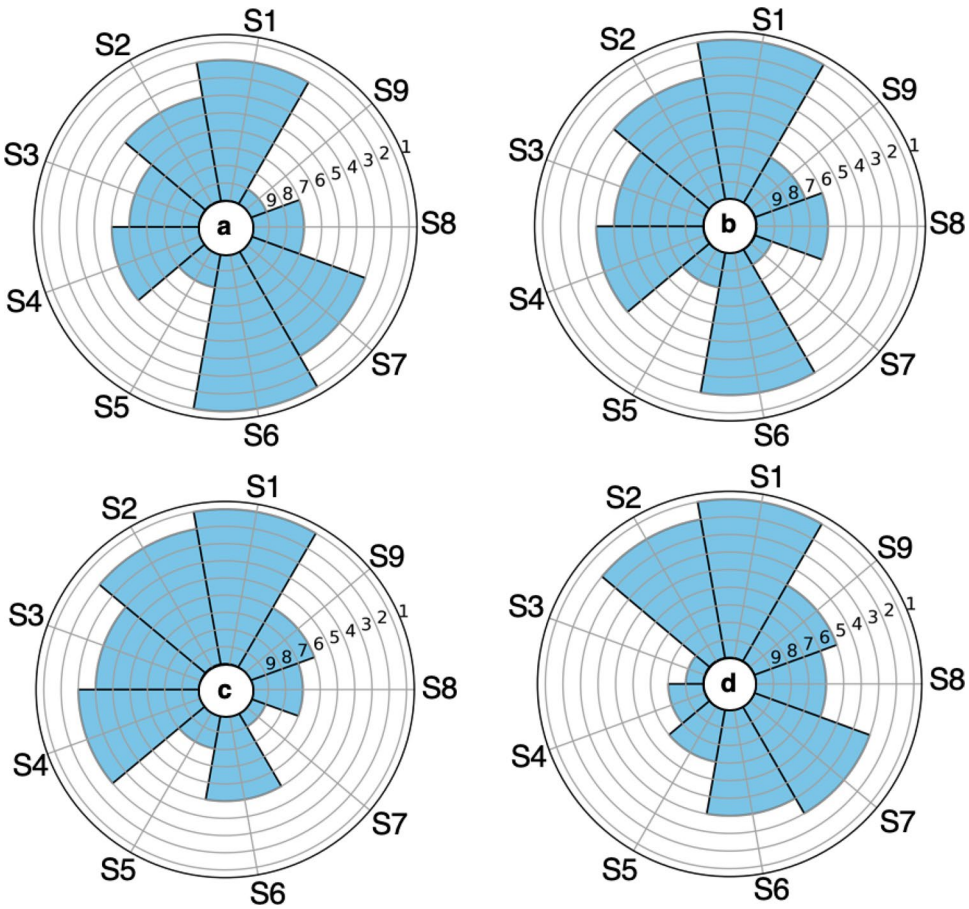

Fig. 9 Sensor-location ranking from best to worst for each model class for the simple-beam example. **a** No-uncertainty scenario; **b** normal-uncertainty scenario; **c** large-uncertainty scenario; **d** very large-uncertainty scenario

4.1.4 Optimal sensor configuration for multiple model classes

In this section, the two methodologies are compared when multiple model classes are plausible. First, a target must be defined for the minimum information gain required for each model class. In this example, although the target is set to 80%, similar results can be found for values such as 70 or 90%.

4.1.4.1 Traditional approach In the union strategy (Fig. 1), the measurement-system design is performed for each model class independently as presented in Sect. 4.1.2. Then the sensor configuration required to reach the target of information gain is defined for each model class. Table 4 presents the sensor selected for each model class to reach 80% of the maximum information gain. These sensor configurations differ by the number of sensors required and selected sensors. In the traditional approach, each sensor that is at least useful for one model class is included in the final sensor configuration. Following this methodology, five sensors (S1, S2, S4, S6, S7) are thus necessary to reach at least 80% of information gain for each model class.

4.1.4.2 Modified hierarchical algorithm The modified hierarchical algorithm (Fig. 3) is modified to design measurement systems for multiple model classes. In this methodology, sensor locations are selected sequentially based on their mean joint-entropy values for all model classes. Figure 10a presents the information gain with respect to the number of sensors. Following this methodology, four sensors are required to reach the 80% target on information gain. Figure 10b shows the sensor-location ranking using the modified hierarchical algorithm. Four sensors are necessary (S1; S2; S3; S5) to reach 80% of the mean information gain for all model classes. Therefore, compared with the traditional approach, a smaller sensor configuration is required following the modified hierarchical algorithm.

Confirmation is needed to verify that 80% of information gain is reached for each model class independently. Table 5 shows the information gain for each model class using the sensor configuration selected by the modified

Table 4 Sensors selected to reach 80% of the maximum information gain for each model class of the simple-beam example

Model class	Sensors selected			
No uncertainty	S1	S2	S6	S7
Normal uncertainty	S1	S2	S4	S6
Large uncertainty	S1	S2	S4	–
Very large uncertainty	S1	–	–	–

This maximum varies with model class

Table 5 Verification that 80% of the maximum information gain is reached for each model class of the simple-beam example

Model class	Total info. gain	80% threshold	Modified hierarchical algorithm
No uncertainty	6.77	5.41	5.42
Normal uncertainty	5.12	4.10	4.27
Large uncertainty	3.48	2.78	3.13
Very large uncertainty	0.56	0.44	0.56

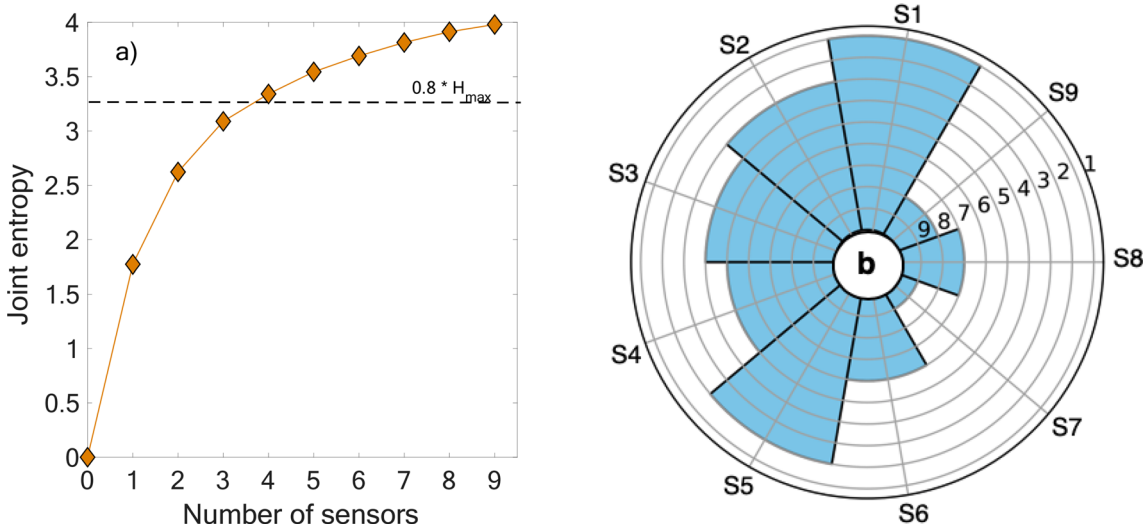

Fig. 10 **a** Joint entropy as a function of the number of sensors for the hierarchical algorithm using multiple model classes. **b** Sensor-location ranking

hierarchical algorithm (Fig. 10) as well as 80% targets. This requirement is fulfilled for each model class. Therefore, this sensor configuration is validated.

4.1.5 Result corroboration: comparison of falsification performance

The falsification performance of selected sensor configurations by the two methodologies (Sect. 4.1.3) is compared. The falsification performance when all possible sensors are included in the configuration is presented as a benchmark in Table 6. For all model classes, results are very similar amongst sensor configurations. The sensor configuration selected by the modified hierarchical algorithm provides a similar information gain of each model class and involves fewer sensors (4 sensors) than the traditional approach (5 sensors). The modified hierarchical algorithm is thus recommended as measurement-system-design methodology when multiple model classes are plausible. This result is verified with a full-scale case study in the next section.

Table 6 Comparison of the falsification performance for the proposed sensor configurations of the simple-beam example

Model class	Falsification performance		
	Traditional approach 5 sensors	Modified hierarchical algorithm 4 sensors	All sensors 9 sensors
No uncertainty	0.96	0.95	0.96
Normal uncertainty	0.90	0.90	0.90
Large uncertainty	0.80	0.79	0.80
Very large uncertainty	0.20	0.20	0.20

4.2 Field application: the powder mill bridge

4.2.1 Bridge and monitoring-system presentation

The Powder Mill Bridge (PMB) (Fig. 11) [57], previously known as the Vernon Avenue Bridge [58], is a steel–concrete bridge located over the Powder Mill pond in Barre (Massachusetts, USA). Built in 2009, the bridge connects the state highway with a depot road that services mainly truck traffic.

The PMB has been monitored since its construction. During the construction, strain gauges, tiltmeters and accelerometers have been installed [58]. The aim of this monitoring was to develop new load-rating procedures for bridge model calibration [57, 59] and to introduce damage-identification methodologies [60, 61]. In 2010 and 2011, dynamic load testing using ambient vibration data has been performed for the purpose of bridge model calibration using a residual-minimization approach [62] and remaining fatigue-life predictions [63].

A quasi-static load test has also been performed in 2011 using a truck of 33 tons that is driven across the bridge at a speed of 3 km/h, which is slow enough to avoid dynamic amplification effects. This data set has not been used in previous studies. The aim of this study is to apply EDMF (Sect. 2.1) and methodologies for measurement-system design (Sect. 3) to the PMB based on this static-test data.

Figure 12 presents the bridge characteristics. PMB is a three-span steel–concrete bridge with a total span of 47 m (Fig. 12a). The concrete deck is supported by six I-section steel girders (Gi) (Fig. 12b). The measurement system and the truck location are shown in Fig. 12c. 20 strain gauges (Si) have been installed on the bottom flange of steel girders to record the structural response during the quasi-static load test and these locations were selected based on engineering judgement. The strain-gauge model is

a) Photograph of the load test

b) Underside of the bridge

Fig. 11 Powder Mill Bridge (PMB) located in Massachusetts, USA

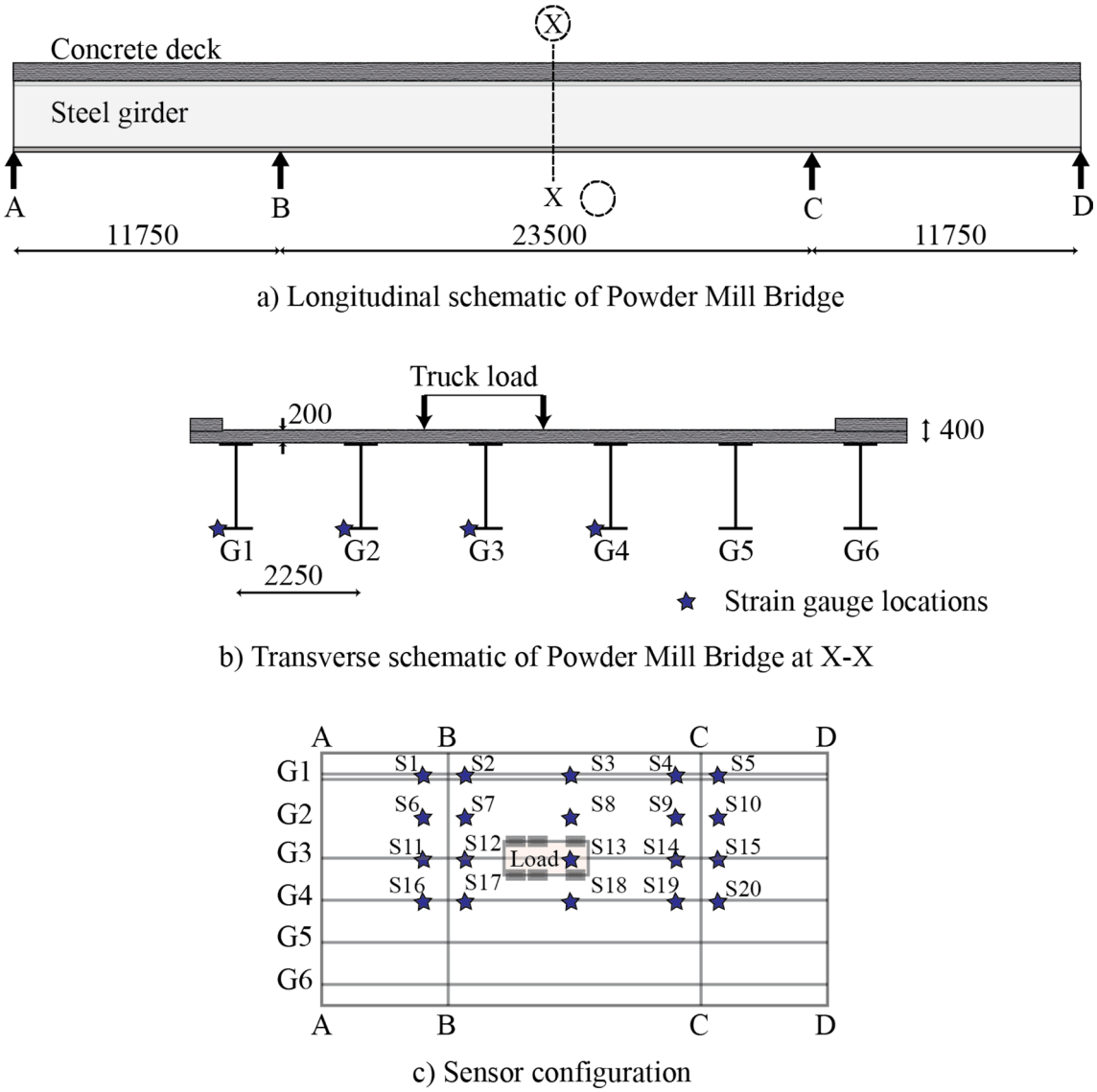

Fig. 12 Schematic drawings of Powder Mill Bridge including installed sensor configuration

KFG-5-120-C1-11L3M3R from the manufacturer Omega [64]. Strain measurements have been recorded at a sampling rate of 200 Hz. Data recorded in the sensors are stored in data loggers installed on the bridge.

The truck position that maximizes strain measurements is considered as the static load test (Fig. 12b, c). Therefore, for each strain gauge, one measurement is used in this study for a total of 20 sensor measurements. The aim of the measurement-system design is thus to evaluate which sensors are useful for model-parameter identification.

4.2.2 Model class selection

A 3D finite-element model is built to interpret strain data. In the numerical model, the concrete deck and steel girders are modelled as homogeneous using shell elements. The footpath on the bridge and the railings have been included to reduce uncertainties.

Table 7 presents the parameters included in the numerical model as well as initial plausible ranges estimated using engineering judgement. The Young's moduli of concrete and steel are parametrized as well as the deck thickness. As the stiffness of the connection between the concrete deck and railings is unknown, the thicknesses of the deck and railing at the edge of the bridge are included as model parameters. Connections between the steel girders and the concrete deck are modelled using zero-length spring elements in both transversal and longitudinal directions. Bridge supports are modelled with zero-length spring elements with parameterized stiffness in longitudinal and vertical directions.

Table 7 Parametric sources of uncertainty in the model and their range

Index	Parameter	Variable	Range
1	Young's modulus of concrete [GPa]	E_C	20–55
2	Young's modulus of steel [GPa]	E_s	195–210
3	Height of deck slab [mm]	H_d	200–210
4	Height of deck slab [mm]	H_r	300–500
5	Deck-girder connection stiffness, transversal [log N/mm]	$K_{dg,x}$	2–6
6	Deck-girder connection stiffness, longitudinal [log N/mm]	$K_{dg,z}$	4–10
7	Vertical stiffness of support A [log N/mm]	$K_{1,y}$	4–7
8	Horizontal stiffness of support A [log N/mm]	$K_{1,z}$	2–5
9	Vertical stiffness of support B [log N/mm]	$K_{2,y}$	4–7
10	Horizontal stiffness of support B [log N/mm]	$K_{2,z}$	2–5
11	Vertical stiffness of support C [log N/mm]	$K_{3,y}$	4–7
12	Horizontal stiffness of support C [log N/mm]	$K_{3,z}$	2–5
13	Vertical stiffness of support D [log N/mm]	$K_{4,y}$	4–7
14	Horizontal stiffness of support D [log N/mm]	$K_{4,z}$	2–5

While 14 parameters have been included in the numerical model, a reduced model-parameter set is needed to cover efficiently the parameter domain with model instances [7]. Typically, 1000 model instances are used for measurement-system design [47]. Two methodologies are used to select the appropriate model class. The development of new methodologies for model-class selection is beyond the scope of this study. Typical methodologies are briefly described below. More details can be found in [13].

The first method involves a traditional sensitivity analysis of model predictions to various parameters conducted using linear regression. As the model-response sensitivity differs between sensor locations, averaged relative influence of each model parameter over the sensor configuration is calculated. Then a practical threshold of 5% is used to select most influent model parameters.

In the second method, called clustering and classification, model responses at sensor locations are first clustered using k-means clustering to understand underlying trends in model response [65]. Clusters are then used to train a support-vector-machine classifier. Parameter selection for the classifier is carried out using forward variable selection. The result of this sequential search is a trade-off plot of classification error as a function of parameters used to train the classifier. This trade-off plot helps determine the model parameters that are informative of structural behavior.

Table 8 presents model parameters selected by both methodologies. The difference between the two model classes is either the absence or presence of the steel Young's modulus. The aim of this paper is not to judge which model class is the most appropriate but rather to consider both as plausible and find the optimal measurement system. The inclusion of this additional parameter can significantly influence the prediction ranges at sensor locations and thus the optimal sensor configuration. Both model classes are taken to be equally likely to be the best model class.

Table 8 Selected model class using linear regression and clustering and classification methods

Model class	Method	Included parameters
Model class 1 (MC1)	Linear regression	E_C, E_s, H_r, $K_{dg,z}$, $K_{2,y}$,$K_{3,y}$
Model class 2 (MC2)	Clustering and classification	E_C, H_r, $K_{dg,z}$, $K_{2,y}$,$K_{3,y}$

Table 9 Non-parametric uncertainty sources – Powder Mill bridge

Source	Distribution
Measurement [%]	N[0; 5]
Load [%]	U[− 5; 5]
Model bias at sensors near supports [%]	U[− 15; 5]
Model bias at sensors near mid-span [%]	U[− 7; 5]
Secondary parameters—model class 1	U[− 17; 20]
Secondary parameters—model class 2	U[− 25; 20]

Table 9 presents uncertainty sources considered in the PMB bridge case study. These sources have been estimated based on engineering judgement, sensitivity analysis and literature review [13]. Measurement uncertainties have been estimated on sensor-supplier information and this source has a normal distribution. Load uncertainties are related to truck weight and position. Model bias is larger close to the support due to the simplification in the numerical model at supports that may affect the accuracy of predictions. The secondary-parameter uncertainty is influenced by the model class used. Uncertainties from these sources are then combined using Monte Carlo sampling.

4.2.3 Measurement-system design for multiple model classes

In this section, the two methodologies for measurement-system design when multiple model classes are plausible are applied to the PMB bridge. Results in terms of joint entropy with respect to the number of sensors and sensor rankings are presented.

Figure 13a presents the joint entropy as a function of the number of sensors for each model class independently. Results show that sensor configurations have similar expected information gain for both model classes. Nevertheless, these sensor configurations may differ in terms of selected sensor locations. To reach the 80% target on information gain, ten sensors are needed for both model classes. As this study has been performed after monitoring, the falsification performance using the field measurements collected during monitoring is shown in Fig. 13b with respect to the number of sensors. S11 and S15 have provided suspicious measurements during monitoring and have thus been removed from the analysis in Fig. 13b. Most model instances have been falsified using the first ten sensors, as predicted by the hierarchical algorithm. However, the comparison between predicted and observed sensor performance is not straightforward since all possible measurement outcomes are taken into account by the hierarchical algorithm [27]. Sensor configurations are thus assessed statistically by the joint-entropy metric while they are evaluated using the true set of measurements by the falsification performance.

Figure 14 presents the sensor-location ranking when each model class is assessed independently. For each model class, results are presented as a histogram with polar coordinates from the first sensor location selected to the last one. For clarity purposes, only the first 10 selected sensors are presented. Most selected sensor locations are the same in the two model classes, for example, S1, S3 or S14. However, rankings differ significantly. Additionally, some locations are only useful for one model class, such as S12 for MC1 or S7 for MC2. This result shows the optimal sensor configuration depends on the model class.

Figure 15a presents the information gain with respect to the number of sensors using the modified hierarchical algorithm and information from both model classes. Following this methodology, eight sensors are required to reach the 80% level of information gain. Figure 15b shows the sensor-location ranking using this methodology. When compared to the traditional approach (Fig. 14), the selected sensor locations are similar while the ranking differs, showing that accounting for mutual information between model classes leads to a unique sensor configuration.

Table 10 presents the selected sensor locations using the traditional approach and the modified hierarchical algorithm to reach a target of information gain fixed at 80%. The same sensor locations are chosen, except that the modified hierarchical algorithm does not select S7 and S10, leading to a smaller monitoring system. This result shows that although the traditional approach selects good sensor locations, it leads to measurement systems with mutual information between sensors. A comparison of these measurement systems in terms of falsification performance is carried out in the next section.

Figure 16 presents the optimal sensor configuration according to the modified hierarchical algorithm. This configuration involves 8 of the 20 possible sensors. Some

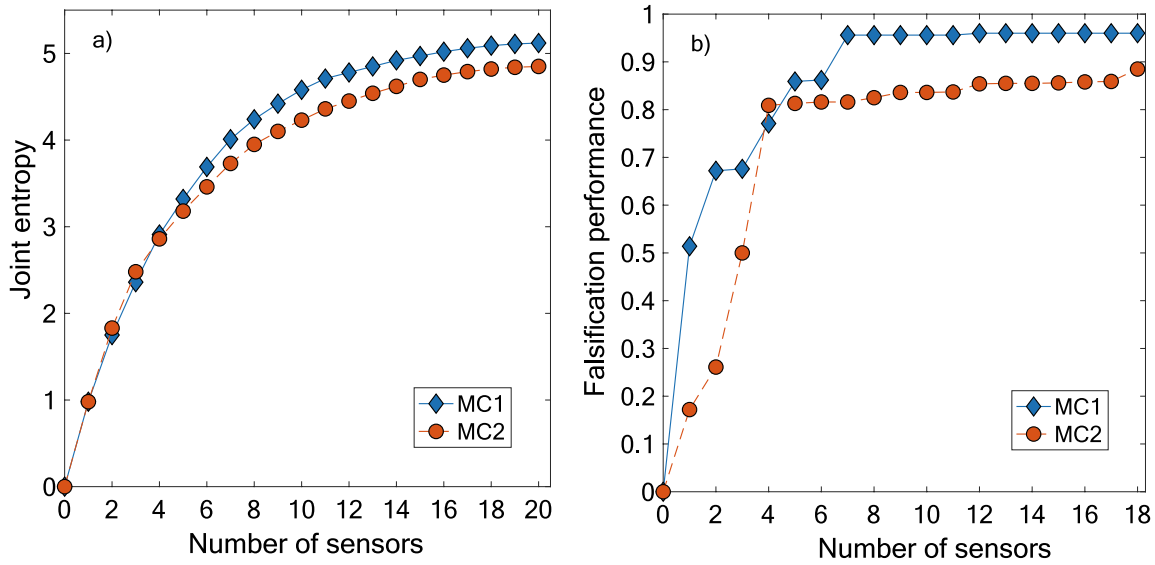

Fig. 13 Comparison of information gain and identification performance with respect to the number of sensors for the two model classes for the PMB bridge. **a** Joint entropy; **b** falsification performance based on field measurements

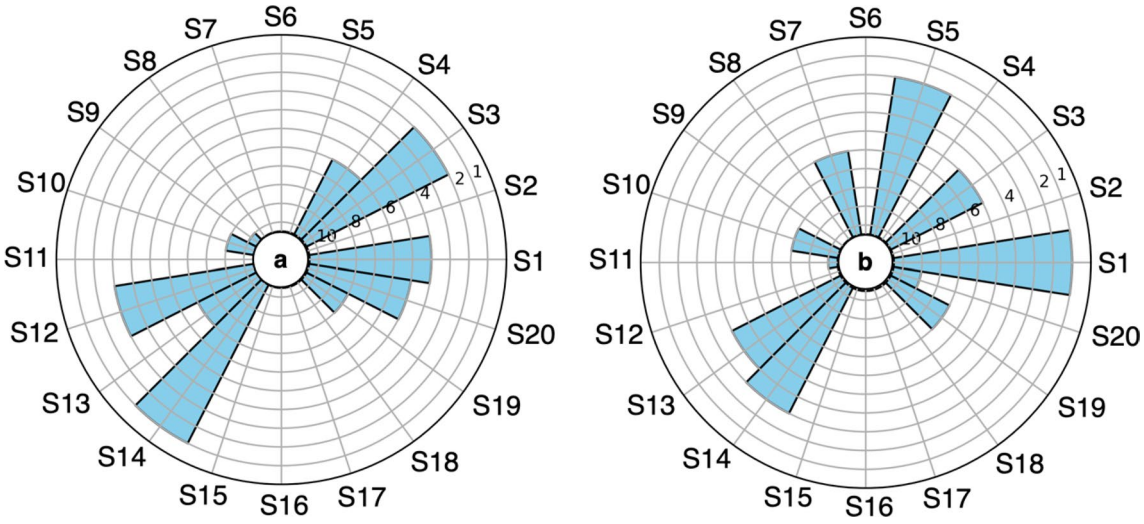

Fig. 14 Sensor-location ranking from best to worst for each model class for the PMB bridge. **a** Linear-regression method (MC1); **b** clustering and classification method (MC2)

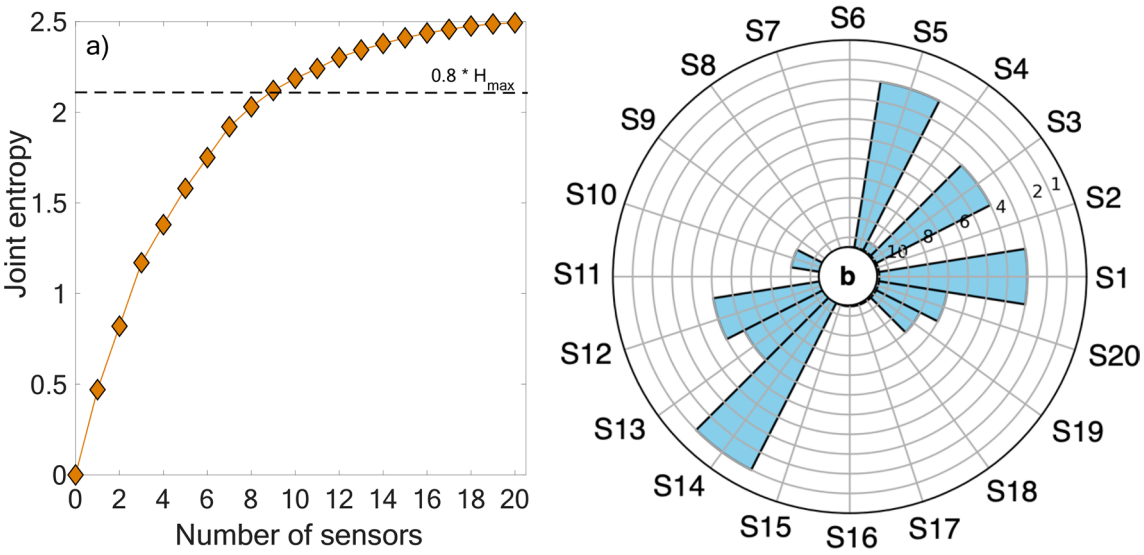

Fig. 15 **a** Joint entropy as a function of the number of sensors for the hierarchical algorithm using multiple model classes. **b** Sensor-location ranking

Table 10 Sensors selected by the two methodologies to reach 80% of the information gain for each model class of the PMB ridge

Methodology	Sensor locations selected									
Traditional approach (MC1)	S1	S3	S5	S7	S10	S12	S13	S14	S19	S20
Modified hierarchical algorithm (MC2)	S1	S3	S5	S12	S13	S14	S19	S20		

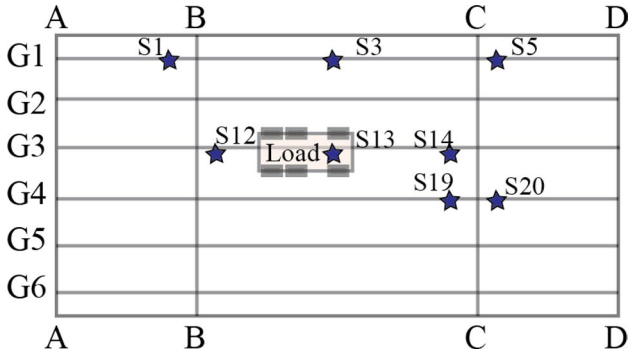

Fig. 16 Optimal solution of the measurement-system design according to the modified hierarchical algorithm

locations correspond to where the signal-to-noise ratio is the highest (S13, S12) but sensors have also been spread over the bridge, such as S1 or S5, showing that the modified hierarchical algorithm does not lead to sensor clustering.

4.2.4 Result corroboration using field measurements

In this section, the falsification performance using field measurements is compared for the sensor configurations that are selected by the two methodologies given multiple model classes (Table 10). Results are presented in Table 11, where the falsification performance when all 18 possible sensors are included in the configuration is included as a benchmark. For all model classes, all sensor configurations lead to similar results. The sensor configuration selected by the modified hierarchical algorithm provides a similar information gain of each model class and involves less sensors (8 sensors) than the union strategy (10 sensors). The modified hierarchical algorithm is thus a better measurement-system-design methodology when multiple model classes are plausible and these results confirm the results that were found for the simple-beam example (Sect. 4.1.4).

5 Discussion

When multiple model classes are plausible, it may occur that some model classes are more likely than others. A strategy to account for this information is to weight sensor entropy values in Eq. (8) in each model class using the probability that this model class is the correct one.

In this study, a target of information gain for each model class is fixed at 80% of the total feasible information gain. This choice has been made as a tradeoff between sufficient information gain and the minimum cost of monitoring. Several target levels (instead of 80%) have been assessed and they lead to the same conclusion that the modified hierarchical algorithm requires fewer sensors to reach the same target level of information gain than required by the traditional approach. Higher target values obviously lead to monitoring systems that include more sensors.

The target used in this paper has been fixed as a percentage of the total information gain. This type of target has been chosen since it can be simply included in a multi-objective approach for measurement-system design, for example [51]. Other types of targets, such as a minimal incremental of the joint entropy are possible without significantly modifying the methodology presented in this study. Although the joint entropy is a monotonic increasing function with respect to the number of sensors, incremental targets may be difficult to define as significant information may be gained by small individual-sensor increments, see for example [49].

The number of sensors that are selected must be sufficient to guarantee that the information gain is sufficient in case of sensor failure. This criterion is not explicitly included in this study. Previous work on single-span bridges [51] shows that typically 5 to 7 sensors in the configuration provide enough mutual information between them to guarantee sufficient information gain even when the most-informative sensor fails.

The following limitations of the work are recognized. The quality of sensor-performance predictions depends upon the quality of the numerical model even though model simplifications can be covered by increased model uncertainty. The reliability of model assumptions must be verified by visual inspection prior to monitoring. Additionally, the inclusion of non-structural elements, such as barriers and asphalt pavement, explicitly in models is recommended to increase the accuracy of model predictions.

The selection of the most relevant model class is a non-trivial task and is an on-going theme of research in many fields. The influence of all relevant parameters on model predictions should be estimated to properly evaluate model

Table 11 Comparison of the falsification performance using field measurements for the proposed sensor configurations on the Powder Mill Bridge

Model class	Falsification performance		
	Traditional approach 10 sensors	Modified hierarchical algorithm 8 sensors	All sensors 18 sensors
Linear regression (MC1)	0.96	0.96	0.96
Clustering and classification (MC2)	0.83	0.84	0.89

uncertainties. In this study, the goal is not to define the single most appropriate model class. Instead, a methodology that accommodates multiple plausible model classes for measurement-system design is proposed.

The hierarchical algorithm uses a greedy search to reduce the computational time required for obtaining optimal sensor placement solutions. As sensor locations are selected sequentially, the global optimum may not be obtained, especially when the selected number of sensors is low. Moreover, the sampling strategy used to generate the population of model predictions may influence the result of the measurement-system design.

Future work includes development of a sensor-placement methodology that requires fewer model-instance predictions without reducing the effectiveness of the measurement-system design.

6 Conclusions

A new methodology is proposed to design measurement systems when multiple model classes are plausible prior to monitoring. This methodology involves a modification of the hierarchical algorithm to account for the information gain of sensor locations over all model classes in the sensor placement. This methodology outperforms the traditional approach on both an illustrative example and a full-scale bridge case study (Powder Mill Bridge, previously known as the Vernon Avenue Bridge). Specific conclusions are the following:

- The optimal configuration depends on the model class chosen by engineers. The proposed strategies help engineers in the design of the optimal measurement systems when multiple model classes are plausible.
- The modified hierarchical algorithm for multiple model classes supports the selection of a sensor configuration that provides significant information gain for each plausible model class.
- This methodology helps reduce the required number of sensors without compromising the precision of model-parameter-value identification after monitoring.

Acknowledgements The research was conducted at the Future Cities Laboratory at the Singapore-ETH Centre, which was established collaboratively between ETH Zurich and Singapore's National Research Foundation (FI 370074011) under its Campus for Research Excellence and Technological Enterprise program. The authors are thankful to M. Sanayei, Tufts University, USA, for providing data related to the Powder Mill Bridge (previously known as the Vernon Avenue Bridge) used in this paper as full-scale application.

Author contributions All authors contributed to the study conception and design. Material preparation, data collection and analysis were performed by Numa Bertola and Sai Pai. The first draft of the manuscript was written by Numa Bertola and all authors commented on previous versions of the manuscript. All authors read and approved the final manuscript.

Funding Open Access funding provided by EPFL Lausanne.

Availability of data and material The following data, models generated or used during the study are available from the corresponding author by request: The model-instance predictions at sensor locations under load-test conditions for both case studies. Results of sensor falsification performance and joint-entropy values.

Compliance with ethical standards

Conflict of interest The authors declare that they have no conflict of interest.

Code availability Open-source codes of the data-interpretation and sensor-placement methodologies are currently under preparation. The GitHub account name is saipai.

References

1. World Economic Forum (2016) Shaping the future of construction, a breakthrough in Mindset and Technology. World Economic Forum, Cologny
2. Hendy CR, Man LS, Mitchell RP, Takano H (2018) Reduced partial factors for assessment in UK assessment standards. In: Proceedings of the Institution of Civil Engineers - Bridge Engineering, vol 171(1), pp 3–1277
3. Catbas F, Kijewski-Correa T, Lynn T, Aktan A (2013) Structural identification of constructed systems. American Society of Civil Engineers, Washington
4. Proverbio M, Vernay DG, Smith IFC (2018) Population-based structural identification for reserve-capacity assessment of existing bridges. J Civil Struct Health Monit 8:1–20
5. Smith IFC (2016) Studies of sensor data interpretation for asset management of the built environment. Front Built Environ 2:2–8
6. Brownjohn JMW, De Stefano A, Xu Y-L et al (2011) Vibration-based monitoring of civil infrastructure: challenges and successes. J Civil Struct Health Monit 1:79–95
7. Saitta S, Kripakaran P, Raphael B, Smith IFC (2010) Feature selection using stochastic search: an application to system identification. J Comput Civ Eng 24:3–10

8. Cheng H, Chen H, Jiang G, Yoshihira K (2007) Nonlinear feature selection by relevance feature vector machine. In: International workshop on machine learning and data mining in pattern recognition, Springer, pp 144–159
9. Friedman JH (1991) Multivariate adaptive regression splines. Ann Stat 19:1–67
10. Matos JC, Cruz PJS, Valente IB et al (2016) An innovative framework for probabilistic-based structural assessment with an application to existing reinforced concrete structures. Eng Struct 111:552–564
11. Pai SG, Reuland Y, Smith IF (2019) Data-interpretation methodologies for practical asset-management. J Sens Actuator Netw 8:36
12. Fan Y, Tang CY (2013) Tuning parameter selection in high dimensional penalized likelihood. J R Stat Soc Ser B 75:531–552
13. Pai SGS, Sanayei M, Smith IFC (2021) Model-class selection using clustering and classification for structural identification and prediction. J Comput Civil Eng 35:04020051
14. Saitta S (2008) Data mining methodologies for supporting engineers during system identification. PhD Thesis n.4056,-EPFL, Lausanne, Switzerland
15. Schlune H, Plos M, Gylltoft K (2009) Improved bridge evaluation through finite element model updating using static and dynamic measurements. Eng Struct 31:1477–1485
16. Beck JL (2010) Bayesian system identification based on probability logic. Struct Control Health Monit 17:825–847
17. Beck JL, Katafygiotis LS (1998) Updating models and their uncertainties. I: Bayesian statistical framework. J Eng Mech 124:455–461
18. Katafygiotis LS, Beck JL (1998) Updating models and their uncertainties. II: model identifiability. J Eng Mech 124:463–467
19. Lam H-F, Yang J, Au S-K (2015) Bayesian model updating of a coupled-slab system using field test data utilizing an enhanced Markov chain Monte Carlo simulation algorithm. Eng Struct 102:144–155
20. Pasquier R, Goulet J-A, Acevedo C, Smith IFC (2014) Improving fatigue evaluations of structures using in-service behavior measurement data. J Bridge Eng 19:04014045
21. Simoen E, Papadimitriou C, Lombaert G (2013) On prediction error correlation in Bayesian model updating. J Sound Vib 332:4136–4152
22. Pai SGS, Nussbaumer A, Smith IFC (2018) Comparing structural identification methodologies for fatigue life prediction of a highway bridge. Front Built Environ 3:73
23. Goulet J-A, Smith IFC (2013) Structural identification with systematic errors and unknown uncertainty dependencies. Comput Struct 128:251–258
24. Popper K (2005) The logic of scientific discovery. Routledge, Abingdon
25. Pasquier R, Smith IFC (2015) Robust system identification and model predictions in the presence of systematic uncertainty. Adv Eng Inform 29:1096–1109
26. Papadimitriou C (2004) Optimal sensor placement methodology for parametric identification of structural systems. J Sound Vib 278:923–947
27. Bertola NJ, Costa A, Smith IFC (2020) Strategy to validate sensor-placement methodologies in the context of sparse measurement in complex urban systems. IEEE Sens J 20:5501–5509
28. Shah PC, Udwadia FE (1978) A methodology for optimal sensor locations for identification of dynamic systems. J Appl Mech 45:188–196
29. Goulet J-A, Smith IFC (2012) Performance-driven measurement system design for structural identification. J Comput Civil Eng 27:427–436
30. Kammer DC (2005) Sensor set expansion for modal vibration testing. Mech Syst Signal Process 19:700–713
31. Papadimitriou C, Beck JL, Au S-K (2000) Entropy-based optimal sensor location for structural model updating. J Vib Control 6:781–800
32. Robert-Nicoud Y, Raphael B, Smith IFC (2005) Configuration of measurement systems using Shannon's entropy function. Comput Struct 83:599–612
33. Kripakaran P, Smith IFC (2009) Configuring and enhancing measurement systems for damage identification. Adv Eng Inform 23:424–432
34. Kammer DC (1991) Sensor placement for on-orbit modal identification and correlation of large space structures. J Guid Control Dyn 14:251–259
35. Sun H, Büyüköztürk O (2015) Optimal sensor placement in structural health monitoring using discrete optimization. Smart Mater Struct 24:125034
36. Raich AM, Liszkai TR (2012) Multi-objective optimization of sensor and excitation layouts for frequency response function-based structural damage identification. Comput Aided Civil Infrastruct Eng 27:95–117
37. Gomes GF, de Almeida FA, da Alexandrino PSL et al (2019) A multiobjective sensor placement optimization for SHM systems considering Fisher information matrix and mode shape interpolation. Eng Comput 35:519–535
38. Yuen K, Kuok S (2015) Efficient Bayesian sensor placement algorithm for structural identification: a general approach for multi-type sensory systems. Earthq Eng Struct Dyn 44:757–774
39. Papadimitriou C, Lombaert G (2012) The effect of prediction error correlation on optimal sensor placement in structural dynamics. Mech Syst Signal Process 28:105–127
40. Zhang Z, Koh C, Duan W (2010) Uniformly sampled genetic algorithm with gradient search for structural identification–Part I: global search. Comput Struct 88:949–962
41. Yi T, Li H, Gu M (2011) Optimal sensor placement for structural health monitoring based on multiple optimization strategies. Struct Des Tall Spec Build 20:881–900
42. Liu W, Gao W, Sun Y, Xu M (2008) Optimal sensor placement for spatial lattice structure based on genetic algorithms. J Sound Vib 317:175–189
43. Kukunuru N, Thella BR, Davuluri RL (2010) Sensor deployment using particle swarm optimization. Int J Eng Sci Technol 2:8
44. Zhang X, Li J, Xing J et al (2014) Optimal sensor placement for latticed shell structure based on an improved particle swarm optimization algorithm. Math Probl Eng 2014:743904
45. Papadopoulou M, Raphael B, Smith IFC, Sekhar C (2014) Hierarchical sensor placement using joint entropy and the effect of modeling error. Entropy 16:5078–5101
46. Papadopoulou M, Raphael B, Smith IFC, Sekhar C (2015) Optimal sensor placement for time-dependent systems: application to wind studies around buildings. J Comput Civil Eng 30:04015024
47. Bertola NJ, Papadopoulou M, Vernay DG, Smith IFC (2017) Optimal multi-type sensor placement for structural identification by static-load testing. Sensors 17:2904
48. Bertola NJ, Smith IFC (2019) A methodology for measurement-system design combining information from static and dynamic excitations for bridge load testing. J Sound Vib 463:114953
49. Bertola NJ, Smith IFC (2019) A comparison of greedy and global searches for measurement-system design in bridge load testing. In: SMAR 2019. Potsdam, pp 1–8
50. Pasquier R, Goulet J-A, Smith IFC (2017) Measurement system design for civil infrastructure using expected utility. Adv Eng Inform 32:40–51
51. Bertola NJ, Cinelli M, Casset S et al (2019) A multi-criteria decision framework to support measurement-system design for bridge load testing. Adv Eng Inform 39:186–202

52. Pasquier R, Smith IFC (2016) Iterative structural identification framework for evaluation of existing structures. Eng Struct 106:179–194
53. Papadimitriou C (2005) Pareto optimal sensor locations for structural identification. Comput Methods Appl Mech Eng 194:1655–1673
54. Robert-Nicoud Y, Raphael B, Smith IFC (2005) System identification through model composition and stochastic search. J Comput Civil Eng 19:239–247
55. Šidák Z (1967) Rectangular confidence regions for the means of multivariate normal distributions. J Am Stat Assoc 62:626–633
56. Krause A, Singh A, Guestrin C (2008) Near-optimal sensor placements in Gaussian processes: theory, efficient algorithms and empirical studies. J Mach Learn Res 9:235–284
57. Bell ES, Lefebvre PJ, Sanayei M et al (2013) Objective load rating of a steel-girder bridge using structural modeling and health monitoring. J Struct Eng 139:1771–1779
58. Sanayei M, Phelps JE, Sipple JD et al (2012) Instrumentation, nondestructive testing, and finite-element model updating for bridge evaluation using strain measurements. J Bridge Eng 17:130–138
59. Sanayei M, Reiff AJ, Brenner BR, Imbaro GR (2016) Load rating of a fully instrumented bridge: comparison of LRFR approaches. J Perform Constr Facil 30:04015019
60. Reiff AJ, Sanayei M, Vogel RM (2016) Statistical bridge damage detection using girder distribution factors. Eng Struct 109:139–151
61. Weinstein JC, Sanayei M, Brenner BR (2018) Bridge damage identification using artificial neural networks. J Bridge Eng 23:04018084
62. Sipple JD, Sanayei M (2015) Full-scale bridge finite-element model calibration using measured frequency-response functions. J Bridge Eng 20:04014103
63. Saberi MR, Rahai AR, Sanayei M, Vogel RM (2016) Bridge fatigue service-life estimation using operational strain measurements. J Bridge Eng 21:04016005
64. Omega Strain-gauge technical data. https://www.omega.com/en-us/resources/strain-gauge-technical-data. Accessed 1 May 2020
65. Tibshirani R, Walther G, Hastie T (2001) Estimating the number of clusters in a data set via the gap statistic. J R Stat Soc Ser B Stat Methodol 63:411–423